Received 28 April 2020; revised 4 June 2020; accepted 5 June 2020. Date of publication 10 June 2020; date of current version 24 June 2020.
The review of this article was arranged by Editor C. Bulucea.

Digital Object Identifier 10.1109/JEDS.2020.3001272

Device Design Guideline for HfO_2-Based Ferroelectric-Gated Nanoelectromechanical System

CHANKEUN YOON (Student Member, IEEE), JINHONG MIN, JAEMIN SHIN (Member, IEEE), AND CHANGHWAN SHIN (Senior Member, IEEE)

Department of Electrical and Computer Engineering, Sungkyunkwan University, Suwon 16419, South Korea

CORRESPONDING AUTHOR: C. SHIN (e-mail: cshin@skku.edu)

This work was supported by the National Research Foundation of Korea (NRF) through a grant funded by the Korean Government (MSIP) under Grant 2020R1A2C1009063.

ABSTRACT Previous studies have suggested that the operating voltage and energy-delay properties of a nanoelectromechanical (NEM) system can be improved using the negative capacitance (NC) effect of ferroelectric materials. However, the advantages of using the NC effects alone have been utilized for perovskite ferroelectric materials, which is incompatible in complementary metal–oxide–semiconductor (CMOS) fabrication processes. In this work, a CMOS-compatible HfO_2-based ferroelectric material is used for the NC + NEM system. The effects of the ferroelectric properties [i.e., remnant polarization (P_r) and coercive field (E_c)] on the NC + NEM system performance are studied in detail. The results show that the NC + NEM system can operate as a relay or a memory device depending on the P_r and E_c values. Moreover, the pull-in/out voltages of the NC + NEM system are more sensitively affected by E_c rather than P_r and decrease as E_c increases. The device design guideline with appropriate P_r and E_c values of the HfO_2-based ferroelectric material is thus developed and discussed to improve the electrical characteristics of NC + NEM relay/memory devices.

INDEX TERMS Coercive field, ferroelectric capacitor, nanoelectromechanical system, negative capacitance, remnant polarization.

I. INTRODUCTION

Scaling the physical/electrical gate lengths of transistors to below a few nanometers has been hampered by their ever-increasing off-state leakage currents. Moreover, this increased leakage current results in degraded energy efficiency [1]; hence, such leakage currents must be addressed for nanometer-scale transistors. To solve this technical problem, a nanoelectromechanical (NEM) system, which has an almost zero off-state leakage current, has received much attention in the electron device community [2]–[4]. The NEM system has been adopted as a logic and memory device because of its steep on/off-state switching behaviors and temperature/radiation-immune operation [5]–[7]. Several recent studies have proposed NEM systems that are connected in series with ferroelectric capacitors (i.e., NC + NEM system) to improve the electrical characteristics of the conventional NEM system [8], [9]. The main idea of the NC + NEM system originated from using the voltage amplification phenomenon achieved by the negative capacitance (NC) effect in ferroelectric layers [10]. In previous studies, the conventional perovskite structure of $Sr_{0.8}Bi_{2.2}Ta_2O_9$ (SBT) was used, but it was incompatible with the complementary metal–oxide–semiconductor (CMOS) fabrication process. Moreover, the minimum required thickness to generate the voltage amplification effect is large enough to be unacceptable for the CMOS fabrication process [11]. Therefore, CMOS-compatible ferroelectric materials should be explored and investigated for the NC + NEM system. From this perspective, the ferroelectricity in hafnium oxide (HfO_2)-based thin films has been discovered and utilized [12] because unlike perovskite-type ferroelectric materials, HfO_2-based ferroelectric materials are compatible with the CMOS fabrication process and have stable ferroelectric

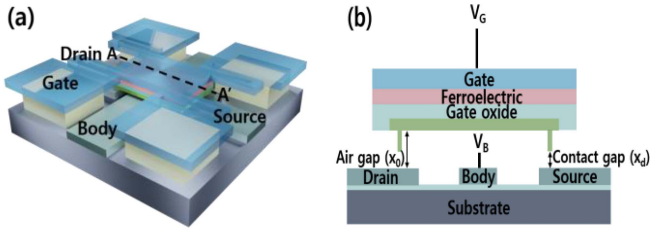

FIGURE 1. (a) Isometric view of the NC + NEM system and (b) cross-sectional view along the AA′ of the NC + NEM system.

characteristics even with nanometer-order thickness (i.e., 5–20 nm) [13], [14]. The representative ferroelectric properties [e.g., coercive field (E_c) and remnant polarization (P_r)] are known to depend on process conditions (e.g., deposition temperature [15], dopants in the materials [16], and thickness of the HfO_2-based ferroelectric films [17]). Therefore, we collected the measured P_r and E_c values of HfO_2-based ferroelectric materials and investigated the effects of the P_r and E_c variations on the NC + NEM system operation. This work specifically presents the range of P_r and E_c, in which the NC + NEM system operates as a logic and memory device. Furthermore, we present the P_r and E_c values that can provide the best device performance for each application. This work would be fruitful in determining the ferroelectric properties for fabricating NC + NEM logic/memory devices.

II. SIMULATION METHODS

Fig. 1 shows the isometric/cross-sectional views of the NC + NEM system. The pull-in state occurs if the sum of the electrostatic (F_{elec}) and adhesion (F_{ad}) forces is stronger than the spring force (F_{spring}) (i.e., $F_{elec} + F_{ad} > F_{spring}$). A movable beam is attached to the bottom electrode if a voltage higher than the pull-in voltage (V_{pi}) is applied to the NEM system, causing a sudden current flow. On the contrary, the pull-out state occurs if the sum of F_{elec} and F_{ad} is weaker than F_{spring} (i.e., $F_{elec} + F_{ad} < F_{spring}$). The attached movable beam is released away from the bottom electrode if a voltage lower than the pull-out voltage (V_{po}) is applied to the NEM system, preventing the flow of current suddenly. In this simulation, gold was used as the metallic conducting channel/electrode to achieve a low surface adhesion force and low operating voltage [18]. Suitable channel/electrode materials for the NC + NEM system should be chosen to improve its electrical performance. In the case of metal-to-metal contacts, the adhesion force is expressed as follows [4]:

$$F_{ad}(x) = 2\gamma A_c \left(\frac{x - D_0}{{\lambda_M}^2}\right) e^{\frac{x-D_0}{\lambda_M}} \quad (1)$$

where γ is the surface energy density; A_c is the contact area; λ_M is the characteristic decay length; D_0 is the average atomic distance when the metal-to-metal contact is formed; and x is the distance between the movable beam and bottom electrodes. The V_{pi} and V_{po} of the NEM system in the pull-in mode is expressed as follows [7]:

$$V_{pi\_NEM} = \sqrt{\frac{8kx_0{}^3}{27\varepsilon_0 A_N}} \quad (2)$$

$$V_{po\_NEM} = \sqrt{\frac{2(x_0 - x_d)^2(kx_d - F_{ad})}{\varepsilon_0 A_N}} \quad (3)$$

where k is the spring constant; x_0 is the air gap; A_N is the actuation area; ε_0 is the dielectric constant of vacuum; and x_d is the contact gap. The switching voltage of a conventional NEM system is high; thus, the NC + NEM system is proposed and designed to implement a much lower switching voltage. The switching voltage of the NC + NEM system in the pull-in mode is expressed as follows [8], [9]:

$$V_{pi\_NCNEM} = \frac{2\alpha_N{}^{EFF}}{3\sqrt{3}} \sqrt{\frac{\alpha_N{}^{EFF}}{\beta_N{}^{EFF}}} \quad (4)$$

$$V_{po\_NCNEM} = \frac{\alpha_N{}^{EFF}}{\alpha_{PI}} V_{po\_NEM} - \frac{\beta_N{}^{EFF}}{\alpha_{PI}{}^3} V_{po\_NEM}^3 \quad (5)$$

where $\alpha_N^{EFF} = \alpha_N - \alpha_F = (kx_0 - F_{ad})/(k\varepsilon_0 A_N) - (-\alpha' t_{FE}/A_{FE})$; $\beta_N{}^{EFF} = \beta_N - \beta_F = 1/(2k(\varepsilon_0 A_N)^2) - \beta' t_{FE}/A_{FE}^3$; $\alpha_{PI} = (x_0 - x_d)/(\varepsilon_0 A_N)$; t_{FE} is the ferroelectric material thickness; A_{FE} is the area of the ferroelectric material; and α' and β' are the ferroelectric anisotropy constants. The NEM system operates in the pull-in mode if the ratio of the contact gap to air gap (x_d/x_0) is greater than 1/3 (i.e., $x_d/x_0 > 1/3$), and vice versa [19]. The air gap is far greater than the contact gap in this simulation (i.e., $x_d/x_0 = 2/3$); hence, the NC + NEM system should still operate in the pull-in mode even if the process-induced variations in the air and contact gaps are considered. The derived switching voltage of the NC + NEM system would therefore remain unchanged and valid. In addition to lowering the switching voltage, the NC + NEM system can be designed to be used not only as a logic device when V_{po} is positive but also as a memory device when V_{po} is negative [Fig. 2(a)] [9], [20]. Moreover, its fabrication process has advantages with regard to deposition of only an additional ferroelectric layer onto the gate oxide layer. Compared to other techniques, such as self-assembled molecular (SAM) coating [21], this is a significant advantage of the NC + NEM system for lowering the operating voltage over that of the conventional NEM system. For simplicity, the ferroelectric anisotropy parameters (i.e., α' and β') were derived from the single-domain Landau–Khalatnikov (L–K) equation as a function of E_c and P_r [22]:

$$\alpha' = -\frac{3\sqrt{3}E_c}{2P_r}, \quad \beta' = \frac{3\sqrt{3}E_c}{2P_r{}^3} \quad (6)$$

However, previous works used a perovskite ferroelectric material [e.g., $Sr_{0.8}Bi_{2.2}Ti_2O_9$ (SBT)] and specific ferroelectric anisotropy constants (i.e., $\alpha' = -6.5 \times 10^7$ m/F, $\beta' = 3.75 \times 10^9$ m^5/C^2F at room temperature). HfO_2-based ferroelectric materials should hence be utilized to fabricate CMOS-compatible NC + NEM systems. We investigated

TABLE 1. Modeling parameters.

Symbol	DESCRIPTION	UNIT	Value
Γ	Surface energy density	J/m^2	1.6
D_0	Average atomic distance	Nm	0.165
λ_M	Characteristic decay length	Nm	0.1
x_0	Air gap	Nm	90
x_d	Contact gap	nm	60
A_N	Actuation area	μm^2	900
A_c	Contact area	nm^2	100
t_{FE}	Thickness of the ferroelectric layer	nm	5.6
A_{FE}	Area of ferroelectric capacitor	μm^2	2
L_{beam}	Beam length	μm	10
t_{beam}	Beam thickness	nm	100
W_{beam}	Beam width	μm	10
E	Young's modulus (Poly-$Si_{0.4}Ge_{0.6}$) [33]	GPa	145
k	Spring constant ($= 32EW_{\text{beam}}t_{\text{beam}}^3/L_{\text{beam}}^3$)	N/m	46.4

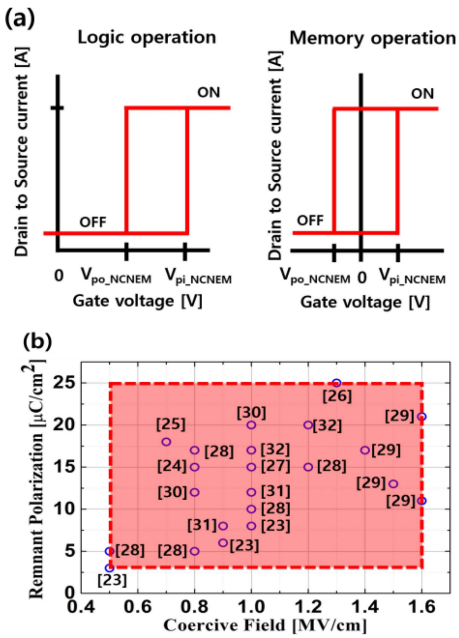

FIGURE 2. (a) Logic/memory operation of the NC + NEM system and (b) measured remnant polarization (P_r) and coercive field (E_c) of the HfO_2-based ferroelectric materials [23]–[32].

the effects of P_r and E_c variations on the NC + NEM system by reviewing published literature [23]–[32] that have reported measured P_r and E_c values of the HfO_2-based ferroelectric material [Fig. 2(b)]. The effects of P_r and E_c variations on the NC + NEM system operation were then investigated by varying P_r and E_c within limited ranges (i.e., 3 μC/cm^2 ≤ P_r ≤ 25 μC/cm^2 and 0.5 MV/cm ≤ E_c ≤ 1.6 MV/cm). A reference/baseline device was designed with the device parameters summarized in Table 1.

III. RESULTS AND DISCUSSION

The NC + NEM system can have two types of operations: (1) effective NEM system mode and (2) effective

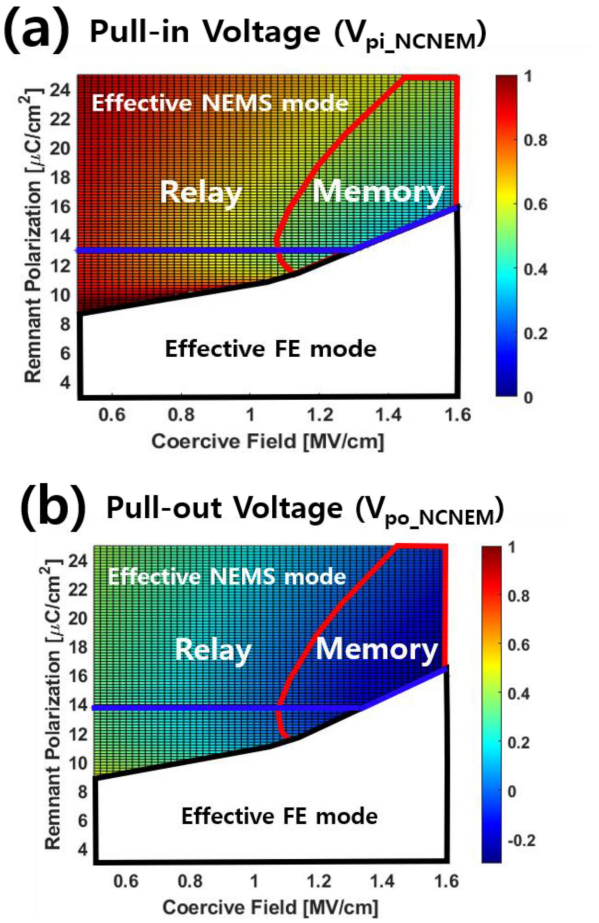

FIGURE 3. (a) Pull-in voltage (V_{pi}) and (b) pull-out voltage (V_{po}) of the NC + NEM system for various remnant polarizations and coercive fields.

ferroelectric (FE) system mode. In the effective NEM system mode, the NC + NEM system operates as a conventional NEM system, wherein α_N^{EFF} and β_N^{EFF} are positive and vice versa [8]. In the effective FE mode, the traveling range of the beam (i.e., distance traveled by the movable beam electrode before it is attached to the bottom electrode) is increased and can be useful for interferometric modulator (IMOD)-based displays [8]. In contrast, the NC + NEM system must operate in the effective NEM system mode to reduce the traveling range of the beam and lower the operating voltage [8]. Therefore, we mapped out the phase space of P_r and E_c and divided it into two regions, where the NC + NEM system operates effectively in the NEM/FE modes. In the effective NEM system mode, if V_{po} is negative, the NC + NEM system is turned on even at zero voltage, indicating that it operates as a nonvolatile memory device. If V_{po} is positive, it operates as a steep switching logic device. Figs. 3(a) and (b) show the pull-in (V_{pi}) and pull-out (V_{po}) voltages of the NC + NEM system, respectively.

According to a previous study, $V_{po} \leq -V_{pi}$ is not desirable because the NEM system would be pulled-in again at reverse charge [8]. This condition did not occur in the present simulation, but special care must be taken to avoid

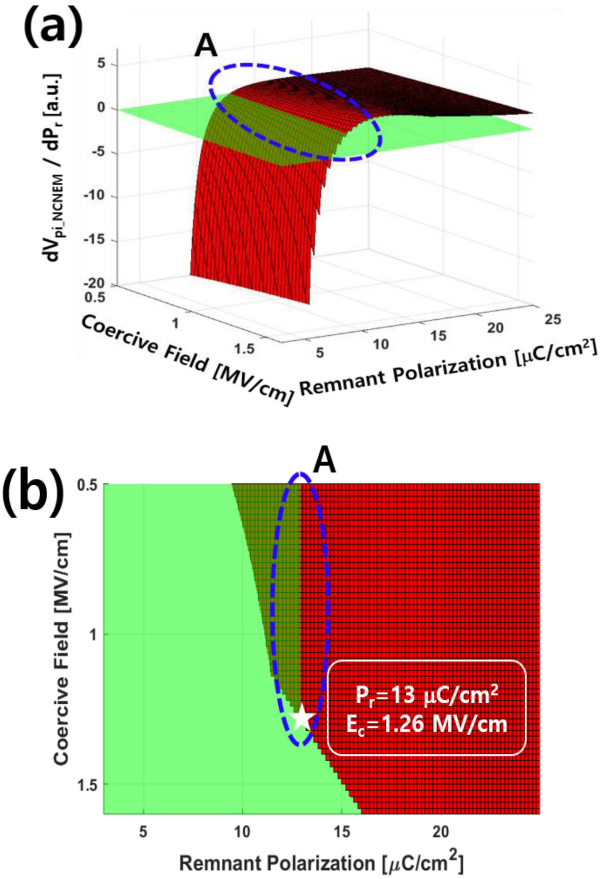

FIGURE 4. **(a) Derivative of the pull-in voltage of the NC + NEM system with respect to the remnant polarization and (b) magnified view of region A.**

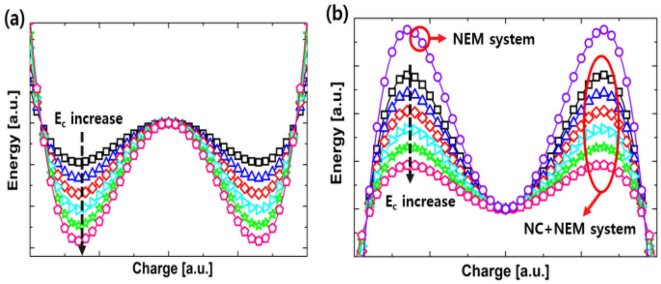

FIGURE 5. **(a) Energy landscapes of the ferroelectric material and (b) energy landscape of the NC + NEM system and reference NEM system for various values of coercive fields.**

this unwanted condition when fabricating the device. The pull-in/out voltages of the NC + NEM system were affected more by the E_c variation than by the P_r variation. The blue-colored line indicates the trend of the minimum pull-in/out voltages of the NC + NEM system. In the case of 8.8 $\mu C/cm^2 \leq P_r \leq 16.6$ $\mu C/cm^2$, V_{pi_NCNEM} decreased as E_c increased until E_c became 1.26 MV/cm. Thereafter, V_{pi_NCNEM} decreased as P_r and E_c increased together. On the contrary, in the case of 16.6 $\mu C/cm^2 \leq P_r \leq 25$ $\mu C/cm^2$, V_{pi_NCNEM} decreased as E_c increased. Fig. 4(a) shows the derivative (or sensitivity) of V_{pi_NCNEM} with respect to P_r for varying P_r and E_c. Fig. 4(a) also indicates that dV_{pi_NCNEM}/dP_r gradually changed from a negative to positive value as P_r increased. The point at which dV_{pi_NCNEM}/dP_r changed from negative to positive is the point at which V_{pi_NCNEM} is minimum. Fig. 4(b) shows a magnified view, where dV_{pi_NCNEM}/dP_r has a zero value. As shown in Fig. 4(b), since dV_{pi_NCNEM}/dP_r changed from a negative to positive value at a certain P_r, V_{pi_NCNEM} had a minimum value at that P_r. Beyond a certain E_c (herein, 1.26 MV/cm), dV_{pi_NCNEM}/dP_r was always positive (Fig. 4). In calculus, if the first-order derivative of f(x) is positive (i.e., df(x)/dx > 0), f(x) increases as x increases. Likewise, V_{pi_NCNEM} increased as P_r increased because dV_{pi_NCNEM}/dP_r was positive beyond a certain E_c (1.26 MV/cm). Therefore, V_{pi_NCNEM} can be reduced by decreasing P_r. However, if P_r becomes too small, the NC + NEM system operates in an effective FE mode (Fig. 3). Hence, when the NC + NEM system operates in the effective NEM mode, the trend for the minimum V_{pi_NCNEM} exists at the boundary between the effective NEM and FE modes beyond a E_c = 1.26 MV/cm. Fig. 5(a) indicates the energy landscape of the ferroelectric material (U_F vs. Q) for various coercive fields (E_c). The minima of the energy landscape reduced as E_c increased. Fig. 5(b) represents the energy landscape of the reference NEM (U_N vs. Q) and NC + NEM (U_{FN} vs. Q) systems. Based on previous studies, the energy landscape of the NC + NEM system was calculated as the sum of the energies of the NEM system and the FE material (i.e., $U_{FN} = U_N + U_F$) [8], [9]. The maxima in the energy landscape of the NC + NEM system were lower than those of the NEM system and further reduced as E_c increased. Hence, the pull-in state of the NC + NEM system can be achieved at a lower gate voltage (i.e., V_{pi_NCNEM} decreases as E_c increases) [9]. Specifically, the pull-in voltage of the conventional NEM system was 1.1215 V. In contrast, the pull-in voltage of the NC + NEM system varied from 0.8415 V to 0.2259 V as E_c increased. For the P_r and E_c variations, the pull-out voltage variations of the NC + NEM system can be understood in the same manner.

The pull-in/out voltage of the NEM system can be adjusted by applying a negative body voltage (V_B) [2], via which the operating voltage (V_{DD}) of the NEM system can be decreased to $V_{pi} - |V_B|$. In the case of the NEM relay, the maximum body voltage was $-V_{po}$ to ensure that the relay turned off at the zero gate voltage. Therefore, the minimum operating voltage (V_{DD}) of the NEM relay was $V_{pi} - V_{po}$ [34]. Meanwhile, the memory window (MW) of the NC + NEM is the voltage difference between V_{pi_NCNEM} and V_{po_NCNEM} (i.e., MW = $V_{pi\_NCNEM} - V_{po\_NCNEM}$). Moreover, a large MW is desirable for a memory device application. Fig. 6 indicates the voltage difference between V_{pi_NCNEM} and V_{po_NCNEM} (i.e., $V_{pi\_NCNEM} - V_{po\_NCNEM}$). The blue-/yellow-colored lines represent the minimum/maximum trends of the

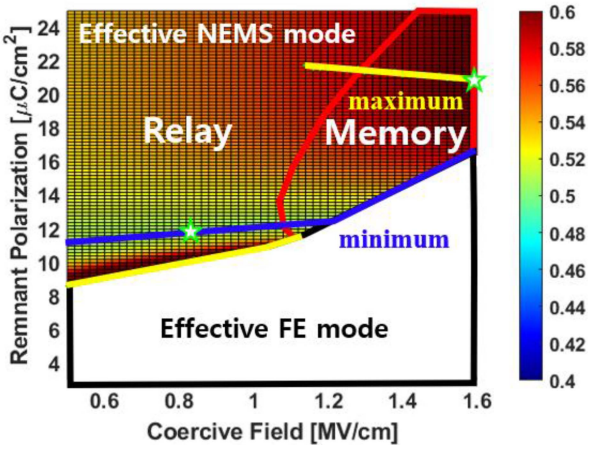

FIGURE 6. Voltage difference between the pull-in/out voltages of the NC + NEM system.

voltage differences between V_{pi_NCNEM} and V_{po_NCNEM} (i.e., $V_{pi\_NCNEM} - V_{po\_NCNEM}$). To operate the NC + NEM relay with a low voltage, the ferroelectric material must have P_r and E_c values on the blue-colored line. Specifically, the lowest operating voltage (i.e., 0.509 V) was obtained when $P_r = 12\ \mu C/cm^2$ and $E_c = 0.86$ MV/cm. On the contrary, the ferroelectric must have P_r and E_c values on the yellow-colored line to operate the NC + NEM with a large MW. Specifically, the largest memory window (i.e., 0.607 V) was achieved when $P_r = 21\ \mu C/cm^2$ and $E_c = 1.6$ MV/cm. Note that the ferroelectric properties of the HfO_2-based ferroelectric material could be varied for any given/identical fabrication process [35]. The ferroelectricity of the HfO_2-based material originated from the formation of a non-centrosymmetric orthorhombic phase [12]. However, in a polycrystalline HfO_2-based ferroelectric material, the orthorhombic phase coexists with the monoclinic or tetragonal phase, which interferes with ferroelectricity. This unwanted variation can be alleviated by fabricating a single-crystalline HfO_2-based ferroelectric material. For the NC + NEM logic/memory device to have minimum operating voltage/maximal memory window, the P_r and E_c values should vary according to the design parameters of the NC + NEM system in this work.

IV. CONCLUSION

The effects of the remnant polarization and the coercive field of the HfO_2-based ferroelectric material on the NC + NEM system were studied herein. Depending on the P_r and E_c values, we theoretically verified that the NC + NEM system could operate as a logic or memory device. The lowest operating voltage of the NC + NEM logic device was theoretically estimated as ~0.5 V when $P_r = 12\ \mu C/cm^2$ and $E_c = 0.86$ MV/cm. The widest memory window (0.607 V) of the NC + NEM memory device was theoretically realized when $P_r = 21\ \mu C/cm^2$ and $E_c = 1.6$ MV/cm. These simulation results are expected to be of guidance for NC + NEM logic/memory devices that can achieve improved electrical characteristics with optimal ferroelectric properties.

REFERENCES

[1] S. Hanson *et al.*, "Ultralow-voltage, minimum-energy CMOS," *IBM J. Res. Develop.*, vol. 50, nos. 4–5, pp. 469–490, Jul. 2006.
[2] R. Nathanael, V. Pott, H. Kam, J. Jeon, and T.-J. K. Liu, "4-terminal relay technology for complementary logic," in *Proc. IEEE Int. Electron Devices Meeting (IEDM)*, Baltimore, MD, USA, 2009, pp. 1–4, doi: 10.1109/IEDM.2009.5424383.
[3] V. Pott, H. Kam, R. Nathanael, J. Jeon, E. Alon, and T.-J. K. Liu, "Mechanical computing redux: Relays for integrated circuit applications," *Proc. IEEE*, vol. 98, no. 12, pp. 2076–2094, Dec. 2010, doi: 10.1109/JPROC.2010.2063411.
[4] I.-R. Chen, C. Qian, E. Yablonovitch, and T.-J. K. Liu, "Nanomechanical switch designs to overcome the surface adhesion energy limit," *IEEE Electron Device Lett.*, vol. 36, no. 9, pp. 963–965, Sep. 2015, doi: 10.1109/LED.2015.2463119.
[5] K. Akarvardar and H. Wong, "Nanoelectromechanical logic and memory devices," *ECS Trans.*, vol. 19, pp. 49–59, May 2009, doi: 10.1149/1.3118930.
[6] W. Y. Choi, "Design and scaling of nano-electro-mechanical non-volatile memory (NEMory) cells," *Current Appl. Phys.*, vol. 10, no. 1, pp. 311–316, Jan. 2010, doi: 10.1016/j.cap.2009.06.014.
[7] H. Kam, T.-J. K. Liu, V. Stojanovic, D. Markovic, and E. Alon, "Design, optimization, and scaling of MEM relays for ultra-low-power digital logic," *IEEE Trans. Electron Devices*, vol. 58, no. 1, pp. 236–250, Jan. 2011, doi: 10.1109/TED.2010.2082545.
[8] M. Masuduzzaman and M. A. Alam, "Effective nanometer air-gap of NEMS devices using negative capacitance of ferroelectric materials," *Nano Lett.*, vol. 14, no. 6, pp. 3160–3165, May 2014, doi: 10.1021/nl5004416.
[9] K. Choe and C. Shin, "Adjusting the operating voltage of an nano-electromechanical relay using negative capacitance," *IEEE Trans. Electron Devices*, vol. 64, no. 12, pp. 5270–5273, Dec. 2017, doi: 10.1109/TED.2017.2756676.
[10] S. Salahuddin and S. Datta, "Use of negative capacitance to provide voltage amplification for low power nanoscale devices," *Nano Lett.*, vol. 8, no. 2, pp. 405–410, Dec. 2007, doi: 10.1021/nl071804g.
[11] G. Pahwa, T. Dutta, A. Agarwal, and Y. S. Chauhan, "Designing energy efficient and hysteresis free negative capacitance FinFET with negative DIBL and 3.5X ION using compact modeling approach," in *Proc. IEEE Eur. Solid-State Circuits Conf. (ESSCIRC)*, Sep. 2016, pp. 49–54, doi: 10.1109/ESSCIRC.2016.7598240.
[12] T. S. Böscke, J. Müller, D. Bräuhaus, U. Schröder, and U. Böttger, "Ferroelectricity in hafnium oxide thin films," *Appl. Phys. Lett.*, vol. 99, no. 10, 2011, Art. no. 102903, doi: 10.1063/1.3634052.
[13] T. S. Böscke, "Crystalline hafnia and zirconia based dielectrics for memory applications," Ph.D. dissertation, Dept. Phys. Elect. Eng. Tech. Univ. Hamburg, Hamburg, Germany, 2010.
[14] E. Yurchuk *et al.*, "Impact of layer thickness on the ferroelectric behaviour of silicon doped hafnium oxide thin films," *Thin Solid Films*, vol. 533, pp. 88–92, Apr. 2013, doi: 10.1016/j.tsf.2012.11.125.
[15] T. Kim, J. Park, B.-H. Cheong, and S. Jeon, "Effects of high pressure nitrogen annealing on ferroelectric $Hf_{0.5}Zr_{0.5}O_2$ films," *Appl. Phys. Lett.*, vol. 112, no. 9, pp. 1–4, Mar. 2018, doi: 10.1063/1.5003369.
[16] S. Starschich and U. Boettger, "An extensive study of the influence of dopants on the ferroelectric properties of HfO_2," *J. Mater. Chem.*, vol. 5, no. 2, pp. 333–338, Jan. 2017, doi: 10.1039/C6TC04807B.
[17] M. H. Park, H. J. Kim, Y. J. Kim, W. Lee, T. Moon, and C. S. Hwang, "Evolution of phases and ferroelectric properties of thin $Hf_{0.5}Zr_{0.5}O_2$ films according to the thickness and annealing temperature," *Appl. Phys. Lett.*, vol. 102, no. 24, pp. 1–5, Jun. 2013, doi: 10.1063/1.4811483.
[18] C. Pawashe, K. Lin, and K. J. Kuhn, "Scaling limits of electrostatic nanorelays," *IEEE Trans. Electron Devices*, vol. 60, no. 9, pp. 2936–2942, Sep. 2013, doi: 10.1109/TED.2013.2273217.
[19] A. Peschot, C. Qian, and T.-J. K. Liu, "Nanoelectromechanical switches for low-power digital computing," *Micromachines*, vol. 6, no. 8, pp. 1046–1065, 2015, doi: 10.3390/mi6081046.
[20] K. Choe and C. Shin, "Ferroelectric-gated nanoelectromechanical non-volatile memory cell," *IEEE Trans. Electron Devices*, vol. 66, no. 1, pp. 407–412, Jan. 2019, doi: 10.1109/TED.2018.2881201.

[21] B. Osoba *et al.*, "Sub-50 mV NEM relay operation enabled by self-assembled molecular coating," in *IEEE Int. Electron Devices Meeting Techn. Dig. (IEDM)*, Dec. 2016, pp. 8–26, doi: 10.1109/IEDM.2016.7838489.

[22] S. Khandelwal, J. P. Duarte, A. I. Khan, S. Salahuddin, and C. Hu, "Impact of parasitic capacitance and ferroelectric parameters on negative capacitance FinFET characteristics," *IEEE Electron Device Lett.*, vol. 38, no. 1, pp. 142–144, Jan. 2017, doi: 10.1109/LED.2016.2628349.

[23] Q. Han *et al.*, "Subthreshold behavior of floating-gate MOSFETs with ferroelectric capacitors," *IEEE Trans. Electron Devices*, vol. 65, no. 10, pp. 4641–4645, Oct. 2018, doi: 10.1109/TED.2018.2863727.

[24] J. Müller *et al.*, "Ferroelectric hafnium oxide: A CMOS-compatible and highly scalable approach to future ferroelectric memories," in *Proc. IEEE Int. Electron Devices Meeting (IEDM)*, Washington, DC, USA, Dec. 2013, pp. 1–4, doi: 10.1109/IEDM.2013.6724605.

[25] J. Müller *et al.*, "Ferroelectric $Zr_{0.5}Hf_{0.5}O_2$ thin films for nonvolatile memory applications," *Appl. Phys. Lett.*, vol. 99, no. 11, Sep. 2011, Art. no. 112901, doi: 10.1063/1.3636417.

[26] M. Kobayashi, N. Ueyama, K. Jang, and T. Hiramoto, "Experimental study on polarization-limited operation speed of negative capacitance FET with ferroelectric HfO_2," in *IEEE Int. Electron Devices Meeting Techn. Dig. (IEDM)*, Dec. 2016, pp. 1–4, doi: 10.1109/IEDM.2016.7838402.

[27] J. Zhou *et al.*, "Ferroelectric HfZrOx Ge and GeSn PMOSFETs with sub-60 mV/decade subthreshold swing, negligible hysteresis, and improved IDS," in *IEEE Int. Electron Devices Meeting Techn. Dig. (IEDM)*, 2016, pp. 1–4, doi: 10.1109/IEDM.2016.7838401.

[28] M. H. Park *et al.*, "Study on the degradation mechanism of the ferroelectric properties of thin $Hf_{0.5}Zr_{0.5}O_2$ films on TiN and Ir electrodes," *Appl. Phys. Lett.*, vol. 105, no. 7, pp. 1–5, Aug. 2014, doi: 10.1063/1.4893376.

[29] T. Kim and S. Jeon, "Pulse switching study on the HfZrO ferroelectric films with high pressure annealing," *IEEE Trans. Electron Devices*, vol. 65, no. 5, pp. 1771–1773, May 2018, doi: 10.1109/TED.2018.2816968.

[30] Y. Li *et al.*, "Negative capacitance oxide thin-film transistor with sub-60 mV/decade subthreshold swing," *IEEE Electron Device Lett.*, vol. 40, no. 5, pp. 826–829, May 2019, doi: 10.1109/LED.2019.2907988.

[31] Y. Goh and S. Jeon, "The effect of the bottom electrode on ferroelectric tunnel junctions based on CMOS-compatible HfO_2," *Nanotechnology*, vol. 29, no. 33, Jun. 2018, Art. no. 335201, doi: 10.1088/1361-6528/aac6b3.

[32] T. Onaya *et al.*, "Ferroelectricity of $Hf_xZr_{1-x}O_2$ thin films fabricated by 300°C low temperature process with plasma-enhanced atomic layer deposition," *Microelectron. Eng.*, vol. 215, pp. 1–5, Jul. 2019, doi: 10.1016/j.mee.2019.111013.

[33] H. Kam and F. Chen, *Micro-Relay Technology for Energy-Efficient Integrated Circuits*. New York, NY, USA: Springer, 2015.

[34] C. Qian, A. Peschot, D. J. Connelly, and T.-J. K. Liu, "Energy-delay performance optimization of NEM logic relay," in *IEEE Int. Electron Devices Meeting Techn. Dig. (IEDM)*, Washington, DC, USA, Dec. 2015, pp. 475–478.

[35] A. T. Bartic, D. J. Wouters, H. E. Maes, J. T. Rickes, and R. M. Waser, "Preisach model for the simulation of ferroelectric capacitors," *J. Appl. Phys.*, vol. 89, pp. 3420–3425, Mar. 2001, doi: 10.1063/1.1335639.